

## Supplementary Text

Generally, GFP-Rac diffuses in the membrane and the signal decay caused by membrane diffusion can be described accurately by a single exponential function (see *Contribution from membrane diffusion*). Let  $k_{\text{diff}}$  be the corresponding apparent rate constant. Then in the presence of membrane diffusion, Eq (1) of the text takes the form:

$$\frac{dc_1}{dt} = -(k_{\text{off}} + k_{\text{diff}})c_1 + k_{\text{on}}c_2. \quad (\text{S1})$$

Given that in all experiments, a signal from the bleached region can be approximated accurately (within a few percent error) by a two-exponential function, we make the substitution,

$$c_2(t) = A \exp(-\alpha t) + B \exp(-\beta t), \quad (\text{S2})$$

after which Eq (S1),  $\frac{dc_1}{dt} = -\gamma c_1 + k_{\text{on}}(Ae^{-\alpha t} + Be^{-\beta t})$  with  $\gamma = k_{\text{off}} + k_{\text{diff}}$ , is integrated readily to yield

$$c_1(t) = c_1(0)e^{-\gamma t} + k_{\text{on}} \left( A \frac{e^{-\alpha t} - e^{-\gamma t}}{\gamma - \alpha} + B \frac{e^{-\beta t} - e^{-\gamma t}}{\gamma - \beta} \right), \quad (\text{S3})$$

where  $c_1(0)$  is the value of  $c_1$  at  $t = 0$ .

Initially  $dc_1/dt = 0$  and  $k_{\text{diff}} = 0$  because at  $t = 0$  the system is at steady state and there is no net membrane diffusion. It then follows from Eqs (S1) and (S2) that  $k_{\text{off}}c_1(0) = k_{\text{on}}c_2(0) = k_{\text{on}}(A + B)$  and

$$k_{\text{on}} = k_{\text{off}}c_1(0)/(A + B) = (\gamma - k_{\text{diff}})c_1(0)/(A + B). \quad (\text{S4})$$

Substituting the right-hand side of Eq (S4) into Eq (S3) for  $k_{\text{on}}$  yields

$$c_{1,\text{norm}}(t) = \frac{c_1(t)}{c_1(0)} = e^{-\gamma t} + (\gamma - k_{\text{diff}}) \left( a \frac{e^{-\alpha t} - e^{-\gamma t}}{\gamma - \alpha} + b \frac{e^{-\beta t} - e^{-\gamma t}}{\gamma - \beta} \right), \quad (\text{S5})$$

where  $a = A/(A+B)$  and  $b = B/(A+B)$  (obviously,  $a + b = 1$ ). With this notation,

$$c_{2,\text{norm}} = \frac{c_2(t)}{c_2(0)} = a \exp(-\alpha t) + b \exp(-\beta t). \quad (\text{S6})$$

Note that in the absence of membrane diffusion,  $k_{\text{diff}} = 0$ ,  $\gamma = k_{\text{off}}$ , and Eq (S5) reduces to Eq (3) of the text.

Fluorescence measured in the unbleached region comes from the membrane and the cytosol. Let  $s$  denote the area of the membrane in the unbleached region that contributes to the signal and  $v$  be volume of the cytosol in the unbleached region that contributes to the signal. Then the full signal is described as  $c_{\text{unbleached}}(t) = c_1(t)s + c_2(t)v$ , and after normalizing to a maximum value at  $t = 0$ ,

$$c_{\text{unbleached, norm}}(t) = \frac{sc_1(t) + vc_2(t)}{sc_1(0) + vc_2(0)} = \frac{c_1(t)}{c_1(0)} \frac{s}{(s + vc_2(0)/c_1(0))} + \frac{c_2(t)}{c_2(0)} \frac{vc_2(0)/c_1(0)}{(s + vc_2(0)/c_1(0))}. \quad (\text{S7})$$

It is convenient to introduce an additional parameter  $r = \frac{s}{s + vc_2(0)/c_1(0)}$  which ranges from 0 at  $s = 0$  (all the signal comes from the cytosol) to 1 at  $v = 0$  (all the signal comes from the membrane). Then Eq (S7) can be rewritten as

$c_{\text{unbleached, norm}}(t) = rc_{1,\text{norm}}(t) + (1-r)c_{2,\text{norm}}(t)$ , and after taking into account Eqs (S5) and (S6),

$$c_{\text{unbleached, norm}}(t) = a(1+r \frac{\alpha - k_{\text{diff}}}{\gamma - \alpha})e^{-\alpha t} + b(1+r \frac{\beta - k_{\text{diff}}}{\gamma - \beta})e^{-\beta t} + r(1-a \frac{\gamma - k_{\text{diff}}}{\gamma - \alpha} - b \frac{\gamma - k_{\text{diff}}}{\gamma - \beta})e^{-\gamma t}. \quad (\text{S8})$$

Note that parameter  $r$  is different from the fraction of the membrane-bound Rac,

$$r_0 = \frac{S}{S + Vc_2(0)/c_1(0)},$$

(where  $V$  and  $S$  are the cell volume and membrane area,

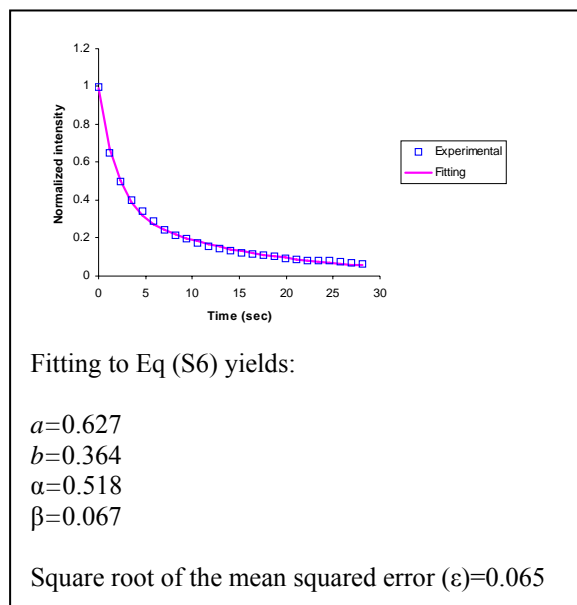
respectively) although follows it qualitatively. In the absence of membrane diffusion ( $k_{\text{diff}} = 0$ ,  $\gamma = k_{\text{off}}$ ), Eq (S8) reduces to the Eq (4) of the text.

Eqs (S6) and (S8) were used in a two-step fitting procedure designed to estimate parameters  $k_{\text{off}}$  and  $r$ . First, the normalized fluorescence decay in the bleached region was fitted to Eq (S6) by varying parameters  $a$ ,  $b$ ,  $\alpha$ ,  $\beta$  constrained by  $a$ ,  $b$ ,  $\alpha$ ,  $\beta > 0$  and  $a + b = 1$ . These values were then used for the second step where the normalized fluorescence decay in the unbleached area was fitted to Eq (S8) by varying parameters  $\gamma$  and  $r$  in the range  $\gamma > 0$  and  $0 < r < 1$ . Parameter  $k_{\text{off}}$  was then determined as  $k_{\text{off}} = \gamma - k_{\text{diff}}$ . In both steps, the least-squares fit was performed with the Microsoft Excel optimization solver. The solver uses the Generalized Reduced Gradient (GRG2) nonlinear optimization algorithm [1], which is a robust version of the Broyden-Fletcher-Goldfarb-Shanno method [2]. Below is an example of the fitting procedure applied to real data:

### **Bleached region**

Time (sec)	Experimental data	Fitting data	Squared error
0	1	0.991	8.1E-05
1.2	0.649928	0.672631899	0.001220281
2.3	0.500717	0.502495686	1.26136E-05
3.5	0.400287	0.390215481	0.000633056
4.7	0.340029	0.320615477	0.003259597

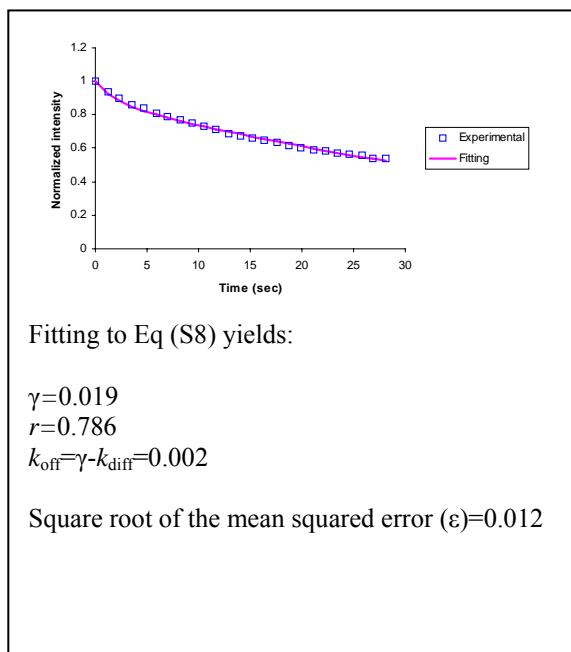
5.9	0.288379	0.274656492	0.002264257
7	0.243902	0.244420724	4.51548E-06
8.2	0.216643	0.21910094	0.000128748
9.4	0.195122	0.198717243	0.000339513
10.5	0.176471	0.182849085	0.001306448
11.7	0.157819	0.167673094	0.003898466
12.9	0.142037	0.154155729	0.007279267
14.1	0.131994	0.14194377	0.005681895
15.2	0.123386	0.131705412	0.004546322
16.4	0.116212	0.121438748	0.002022565
17.6	0.111908	0.112007824	7.92865E-07
18.7	0.104735	0.104024693	4.59404E-05
19.9	0.093257	0.095973472	0.000848611
21.1	0.088953	0.088551184	2.03699E-05
22.3	0.083214	0.081706022	0.000328298
23.4	0.080344	0.075898645	0.003061734
24.6	0.080344	0.070033944	0.016467952
25.8	0.074605	0.064622917	0.017903607
26.9	0.068867	0.060031123	0.016460395
28.1	0.064562	0.055393334	0.02016934



### Unbleached region

Values of parameters  $a$ ,  $b$ ,  $\alpha$ ,  $\beta$  (shown above) were kept constant when fitting the normalized fluorescence decay in the unbleached area to Eq (S8).

Time (sec)	Experimental data	Fitting data	Squared error
0	1	0.998075354	3.7E-06
1.2	0.938317757	0.926600431	0.000156
2.3	0.899065421	0.883186426	0.000312
3.5	0.857943925	0.849119208	0.000106
4.7	0.841121495	0.8227785	0.000476
5.9	0.809345794	0.800718517	0.000114
7	0.788785047	0.782660847	6.03E-05
8.2	0.768224299	0.76437649	2.51E-05
9.4	0.747663551	0.747031935	7.14E-07
10.5	0.730841121	0.731698753	1.38E-06
11.7	0.710280374	0.71543526	5.27E-05
12.9	0.687850467	0.699568014	0.00029
14.1	0.676635514	0.684047556	0.00012
15.2	0.657943925	0.670101703	0.000341
16.4	0.65046729	0.655180281	5.25E-05
17.6	0.63364486	0.640554653	0.000119
18.7	0.618691589	0.627402372	0.000198
19.9	0.603738318	0.613327881	0.000252
21.1	0.592523364	0.599535085	0.00014
22.3	0.58317757	0.586020562	2.38E-05
23.4	0.571962617	0.573873861	1.12E-05
24.6	0.564485981	0.560883363	4.07E-05
25.8	0.558878505	0.548161293	0.000368



26.9 0.542056075 0.53673218 9.65E-05  
 28.1 0.540186916 0.524514608 0.000842

The overall reliability of the proposed method depends on sensitivity of the least-squares fit to parameter changes and validity of the compartmental approximation. While remaining within the compartmental approximation, one can estimate accuracy with which the solver recovers values of  $k_{\text{off}}$  and  $r$  in the presence of noise mimicking measurement error. Specifically, 15% -amplitude noise was superimposed on “data” generated by Eq (S5) and Eq (S6) for certain representative parameter sets (see Supplementary Figure 1, *a-c*). The “data” were then subject to the fitting procedure as described above. Test results, summarized in Table below, indicate that  $k_{\text{off}}$  values are recovered within 3-6% error which is comparable with the error of fit whereas the relative error of  $r$  values is roughly twice as large. Remarkably,

**Table. Test results**

**Data set**

#	Fitting error, %	$k_{\text{off}}$	$r$	
1	4.3	0.03	0.5	
		0.0312	0.5390	recovered values
2	3.8	3.8	7.8	error, %
		0.02	0.6667	
3	3.9	0.0208	0.7271	recovered values
		4.2	9.1	error, %
3	3.9	0.07	0.6667	
		0.0745	0.7625	recovered values
		6.4	14.4	error, %

the method is sensitive enough to distinguish between two parameter sets, #1 and #3, that produce similar fluorescent decays in the unbleached area as shown in Supplementary Figure 1, *a* and *c*.

Validation of the compartmental approximation based on the assumption of fast cytosolic diffusion over the width of the unbleached region compared to the interaction with the membrane is more complicated. For this, “data” should be generated from spatial simulations on realistic three-dimensional (3D) geometry where diffusion in the cytosol is explicitly taken into account and coupled to diffusion in the membrane. Realistic 3D geometry is also necessary to model varying bleaching efficiency in the out-of-focus planes. To run spatial simulations, an appropriate range for the diffusion coefficient of the cytosolic GFP-Rac should be used. According to estimates and recent measurements [3], the diffusion coefficient of a 50-kDa cytosolic protein is around 20  $\mu\text{m}^2/\text{sec}$ . Taking all these into account, we have simulated the FLIP protocol in 3D using the Virtual Cell (a detailed description of the model is beyond the scope of this paper and will be published elsewhere). Results are shown in Supplementary Figure 2 for some representative parameter sets. Again, the “data” generated from the spatial simulations were subject to the fitting procedure. Interestingly, as in the experiments, the simulated “bleached” data were fitted well to the two-exponential function in all cases. Overall, the estimates of  $k_{\text{off}}$  and  $r$  obtained through the fitting procedure follow the changes introduced in the model although the compartmental approximation tends to

underestimate  $k_{\text{off}}$  at higher fractions of the membrane-bound Rac  $r_0$  because tight binding effectively slows down diffusion in the cytosol.

### References.

1. Liebman, J., Lasdon, L. S., Schrage, L., and Waren, A. D. Modeling and Optimization with GINO. The Scientific Press, Palo Alto, CA, 1986.
2. Press, W. H., Teukolsky, S. A., Vetterling, W.T., Flannery, B. P. Numerical Recipes in C: The Art of Scientific Computing. 2<sup>nd</sup> ed. Cambridge University Press, Cambridge, UK, 1999.
3. Arrio-Dupont, M., Foucault, G., Vacher, M., Devaux, P. E., Cribier, S. Translational Diffusion of Globular Proteins in the Cyttoplasm of Cultured Muscle Cells. *Biophys. J.* **78**: 901-907, 2000.

### Legends for Supplementary Figures

Supplementary Figure 1. Sensitivity of the method to parameter changes in the presence of noise. The fitting procedure as described in the text was applied to “data” generated in the presence of noise by Eqs (S5) and (S6) for representative parameter sets. Measurement error mimicked by the superimposed noise is 15%.

Supplementary Figure 2. Validation of the compartmental approximation. “Data” are generated from realistic simulations performed on 3D cell geometry taken from experimental images. The cell geometry used in the simulations has an overall surface-to-volume ratio of  $0.524 \mu\text{m}^{-1}$  whereas the surface-to-volume ratio of the unbleached region is  $0.828 \mu\text{m}^{-1}$ , hence  $r$  values are greater than the corresponding  $r_0$ 's. The diffusion coefficients in the cytosol and in the membrane are  $20 \mu\text{m}^2/\text{sec}$  and  $0.25 \mu\text{m}^2/\text{sec}$ , respectively, and the corresponding  $k_{\text{diff}}$  is  $0.0352 \text{ s}^{-1}$ .

Supplementary Figure 3. Geometry of protrusions. Representative cells expressing the indicated constructs were imaged under the same experimental conditions used for photobleaching. Arrowheads point to typical protrusive areas. Z profiles (lower panel) were acquired across a vertical plane defined by the white lines. The optical slice is  $1 \mu\text{m}$  and the spatial interval is  $1 \mu\text{m}$ . Scale bar is  $20 \mu\text{m}$ .

Supplementary Figure 4. Effect of Rac regulators on Rac activation. Lysates from NIH3T3 cells transfected with the indicated constructs were incubated with GST-PBD and bound, active GFP-Rac was detected by immunoblotting. Lysates were also probed for total GFP-Rac and RhoGDI. Numbers indicate levels of active Rac normalized to total Rac. Amount of active Rac in RhoGDI RNAi-treated cells was expressed relative to that in control RNAi-treated cells (arbitrarily set to 1). Amount of active Rac in all other conditions was expressed relative to that in cells transfected with GFP-wtRac (also set to 1). Vertical lines indicate that samples were run in the same SDS-PAGE gel. Data are representative of three independent experiments.

### Supplementary Materials and Methods

**Active Rac pull-down assays**

Cells were chilled on ice, washed with ice-cold Tris-buffered saline (TBS) and lysed in buffer containing 50 mM Tris pH 7.4, 500 mM NaCl, 10 mM MgCl<sub>2</sub>, 1% Triton X-100, 0.1% SDS, 0.5% sodium deoxycholate, a cocktail of protease inhibitors (Sigma) and 20µg of recombinant GST-PBD. Clarified lysates were then incubated with Glutathione-Sepharose 4B beads (Amersham Biosciences) for 30 min at 4°C and beads were washed with lysis buffer, followed by elution with sample buffer. Bound and total GFP-Rac were analyzed by immunoblotting using the B-2 monoclonal anti-GFP antibody (Santa Cruz Biotechnology).